

Anomalous transport and localization in periodic dissipatively coupled photonic chains

I. Peshko,¹ G. Ya. Slepyan,² and D. Mogilevtsev¹

¹*B.I.Stepanov Institute of Physics, NAS of Belarus, Nezavisimosti ave. 68, 220072 Minsk, Belarus*

²*School of Electrical Engineering, Tel Aviv University, Tel Aviv 69978, Israel*

(Dated: July 2022)

Here we show that coherent random walk in a perfectly periodic chain of dissipatively coupled bosonic modes can exhibit a variety of different anomalous transfer regimes in dependence on the initial state of the chain. In particular, for any given finite initial time-interval there is a set of initial states leading to hyper-ballistic transport regime. Also, there are initial states allowing to achieve a sub-diffusive regime or even localization for a given time-interval, or change asymptotic long-time diffusion rate. We show how these anomalous transport regimes can be practically realized in a planar system of coupled single-mode waveguides with designed loss.

I. INTRODUCTION

Quantum walks are already for quite a long time an intensively pursued field of research^{1–4}. Their time-continuous version represents a general scheme of quantum state transport through a network of coupled quantum systems, and can be used for consideration of numerous transport phenomena in solid-state physics, biophysics, photonic etc.^{2,5–11}. Typically, in absence of decoherence and loss, quantum walks demonstrate ballistic spatial spread in difference with classical random walks demonstrating diffusive spread². Spatial variance behaviour can be altered in a number of ways toward hyper-ballistic, or sub-diffusive regimes, or even localization, for example, by randomly perturbing network and making the structure non-homogeneous, or via nonlinear walks, or controlled time-dependent operations, or by subjecting the network to non-Markovian noise making probabilities of jumps between the network systems time-dependent^{12–18}.

Decoherence and loss can also drastically influence the transport regime, in particular, turning quantum walk into the classical one and switching the ballistic regime to the diffusive one after some interaction time even in perfectly periodic lattices^{3,19–22}.

Here we make a step further and demonstrate that in lattices with dissipative coupling, i.e., when sites are connected with each other only through a common dissipative reservoir, even in a perfectly periodic 1D chain of bosonic modes one can widely vary transport behaviour just by choosing an initial state of the modes. In particular, for an arbitrary finite time interval one can achieve super-ballistic growth of a spatial variance, or sub-diffusive and even localization behavior. For the considered cases, an asymptotic behaviour always remains diffusive. However, the rate of diffusion depends on the initial state.

We suggest a way of practical realization of the discussed coherent walk scheme with a system of dissipatively coupled single-mode waveguides and demonstrate that the discussed transport regimes are feasible in realistic systems of unitary coupled waveguides with engineered local loss.

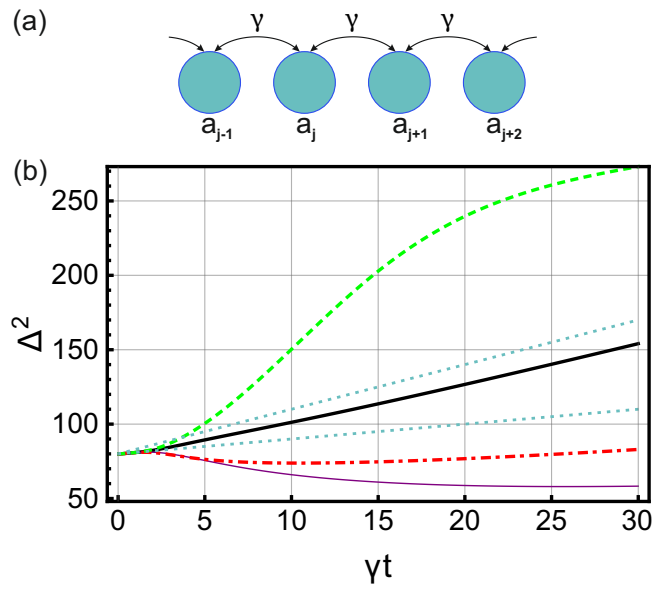


FIG. 1. (a) The scheme of dissipatively coupled tight-binding chain of bosonic modes described by Eq.(2). (b) The variance for the initial state given by Eq.(5) for the four initially excited modes with the numbers $k = n_0 - 8, n_0, n_0 + 8, n_0 + 16$ for $n_0 = 150$ in the chain with 300 waveguides. Thick solid, thin solid, dashed and dash-dotted lines correspond to the following state signatures: $\{+, +, -, -\}$, $\{+, -, -, -\}$, $\{+, +, +, +\}$, $\{-, +, -, +\}$. Upper and lower dotted lines correspond to the linear dependencies $3\gamma t$ and γt .

II. MODEL

We start with the following master equation describing the system of dissipatively coupled bosonic modes schematically shown in Fig.1 (a):

$$\frac{d}{dt}\rho = \sum_{\forall j} \gamma(2L_j\rho L_j^\dagger - \rho L_j^\dagger L_j - L_j^\dagger L_j\rho), \quad (1)$$

where γ is the dissipation rate and the Lindblad operators $L_j = a_j + a_{j+1}$ describe symmetric next-neighbor dissipative coupling between j -th and $j + 1$ -th modes

with the annihilation operators a_j and a_{j+1} . Such system where considered as a basis for coherent diffusive photonics for building equalizers and distributors, non-reciprocal optical circuits, non-classical state protection and generation^{23–27}. Adding unitary coupling between modes and adjusting dissipative coupling between the modes, one can achieve unidirectional field transfer along the chain and create topologically non-trivial bound states^{24,28}. But even in the simplest purely dissipative form Eq.(1) leads to a number of quite unusual transport regimes.

III. SOLUTION

Let us consider how the energy flows through our set of bosonic modes. To that end we consider the equation for the first-order correlation functions $g_{j,k}(t) = \langle a_j^\dagger(t)a_k(t) \rangle$ following from Eq.(1):

$$\frac{1}{\gamma} \frac{d}{dt} g_{j,k} = -4g_{j,k} - g_{j+1,k} - g_{j-1,k} - g_{j,k+1} - g_{j,k-1} \quad (2)$$

and the normalized population distribution

$$p_j = \frac{g_{j,j}}{p_{tot}}, \quad p_{tot} = \sum_{\forall j} g_{j,j}. \quad (3)$$

Further we assume the case when the initially excited modes are far from the edges of the chain and during the time-interval of our interest excitation is still far from the edges. We consider the dynamics of the excitation spread through the modes described by the variance $\Delta^2(t)$

$$\Delta^2 = \sum_{\forall j} (j - \bar{x})^2 p_j, \quad \bar{x} = \sum_{\forall j} j p_j, \quad (4)$$

where \bar{x} is the average time-dependent excitation shift. Notice that by a trivial sign change

$$g_{j,k} \rightarrow (-1)^{j+k} g_{j,k}$$

Eq.(2) transforms to the equation formally coinciding with the one describing a 2D classical continuous random walk^{2,29}. Thus, for the 1D chain of finite length described by Eq.(2), the exact solution can be easily found^{29,30} for any initial set of $g_{j,k}$. Notice, however, that in difference with the classical random walk, $g_{j,k}$ are complex-values functions. In the space-continuous regime (i.e, when the discrete number of the mode is changes to continuous variable) Eq.(2) describes coherent diffusion of field spatial coherence^{31,32}. Such coherent diffusion of a complex-valued fields can be found also in other fields of physics, for example, when studying atomic coherence in a gas of diffusing atoms^{33,34}, or restricted diffusion in a magnetic field³⁵, or spin-transport in semiconductors³⁶.

IV. REGIMES

To give a gist of what kind of transport one can get from Eq.(2), let us consider a case when only some set

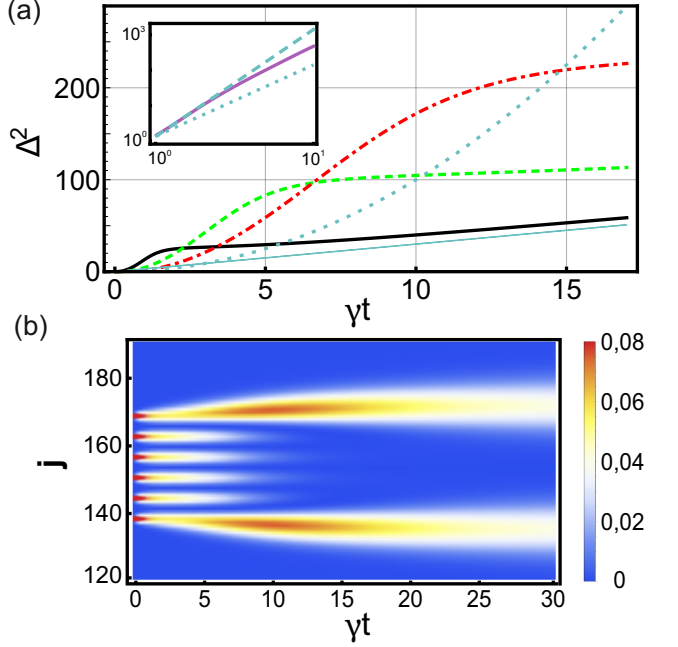


FIG. 2. (a) Illustration of the super-ballistic regime scaling for the initial state given by Eq.(6). Thick solid, dashed and dash-dotted lines correspond to $m = 1, 2, 3$ and the function $\Delta^2(t) - \Delta^2(0)$. The thin solid line corresponds to the diffusive regime $\Delta^2(t) = 3\gamma t$. The dotted line shows the ballistic regime $\Delta^2(t) = \gamma^2 t^2$. The inset shows log-log plots of the variance given by Eq.(7). In the inset the dashed and dotted lines show the super-ballistic and ballistic regimes given by $\Delta^2(t) = 1.4(\gamma t)^n$, $n = 3, 2$. (b) The distribution of $p_j(t)$ for the initial state corresponding to $m = 3$. Other parameters are as for Fig. 1(b).

of modes $\{k\}$ are initially excited in coherent states with equal absolute amplitudes but with different combinations of possible π -differences in phase, whereas all the other modes are initially in the vacuum state:

$$\rho(0) = |\psi\rangle\langle\psi|, \quad |\psi\rangle = \prod_{\forall k} |\delta_k \alpha_k\rangle \prod_{\forall j \neq k} |0\rangle_j, \quad (5)$$

where $\delta_k = \pm 1$. Fig. 1(b) shows the variance, $\Delta^2(t)$ of Eq.(4) for the case of four modes being initially excited, $k = n_0 - 2m, n_0, n_0 + 2m, n_0 + 4m$, where n_0 is the number of the system in the middle of the chain, $m = 4$, and $\alpha = 1$. One can see that the choice of δ_k can drastically affect the transport dynamics. First of all, the result of the signature choice, $\text{sign}[\delta_{1,2,3,4}] = \{+, +, -, -\}$, shown by the thick solid curve in Fig. 1(b) gives an intuitively expected linear diffusive regime for times exceeding a typical interaction time-scale ($\gamma t > 1$), but with an unexpected rate: 3γ instead of classically expected γ (upper dotted line shows the dependence $\Delta^2(t) = 3\gamma t$). The signature $\{+, +, +, +\}$ gives an expected linear diffusive regime with the rate γ shown by the dash-dotted curve in Fig. 1(b) (for comparison, the lower dotted line shows the dependence $\Delta^2(t) = \gamma t$). However, the variance

comes to this regime only after some period of lowering the variance, and the length of this regime significantly exceeds the inverse rate, γ^{-1} . Moreover, the signature $\{+, -, -, -\}$ gives only the localization, i.e., the variance only diminishes during the considered interaction time (as shown by the thin solid line in Fig. 1(b)). Finally, the signature $\{-, +, -, +\}$ leads to a faster than diffusive transport regime (the dashed curve in Fig. 1(b)).

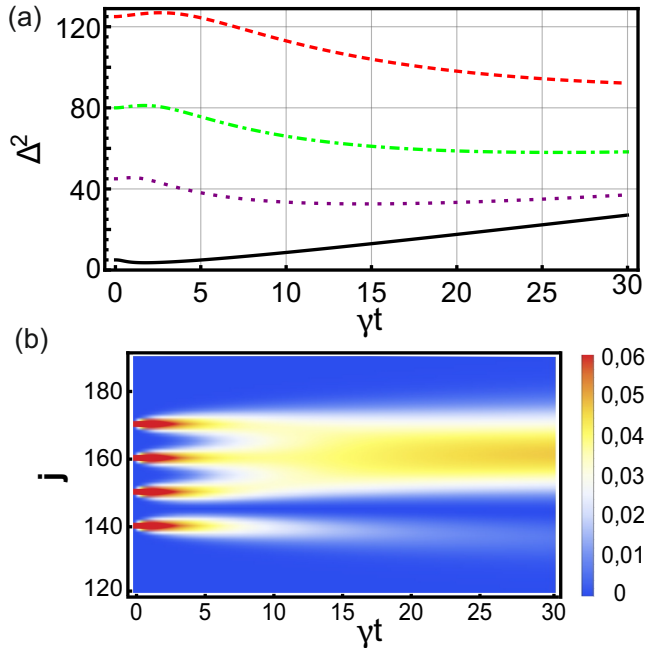


FIG. 3. (a). Scaling of the localization regime for the initial state (5) with 4 initially excited modes with numbers $k = n_0 - 2m, n_0, n_0 + 2m, n_0 + 4m$ and the signature $\{+, -, -, -\}$. Solid, dotted, dash-dotted and dashed lines correspond to $m = 1, 3, 4, 5$. (b) The distribution of $p_j(t)$ for the initial state corresponding to $m = 5$. Other parameters are as for Fig. (1)(b).

V. SUPER-BALLISTIC REGIME AND SCALING

Now let us show that the faster-than-diffusive regime exemplified by the dashed curve in Fig. 1(b)) can be super-ballistic. Also, it can be scaled up. I.e., by choice of the initial state one can get a super-ballistic transport for any given time-interval for $\gamma t > 1$ and extend it to an arbitrary time-interval. This case is illustrated in the main panel of Fig. 2(a). Here the variance dynamics is given for the state (5) with six initially excited modes with the numbers

$$k = n_0 - 4m, n_0 - 2m, n_0, n_0 + 2m, n_0 + 4m, n_0 + 6m \quad (6)$$

with the amplitude $\alpha = 1$ and the signature $\{-, +, -, +, -, +\}$. Thick solid, dashed and dash-dotted

lines correspond to $m = 1, 2, 3$. For comparison, the diffusive regime $\Delta^2(t) = 3\gamma t$ is shown by the thin solid line, and the ballistic $\Delta^2(t) = \gamma^2 t^2$ is shown by the dotted line; for better comparison the values of $\Delta^2(t) - \Delta^2(0)$ were shown for each case. One can see how the super-ballistic region extends toward longer interaction times with increasing of the localization region of the initial state. The inset in Fig. 2 plotted in log-log axes shows that there is indeed an extended (i.e., for several γt intervals) super-ballistic stage in dynamics, and it can have a stage when $\Delta^2(t) \propto (\gamma t)^3$. The dotted line in the inset corresponds to $\Delta^2(t) \approx 1.4(\gamma t)^2$, the dashed line corresponds to $\Delta^2(t) \approx 1.4(\gamma t)^3$. The solid line in the inset corresponds to the initial state (5) with twelve initially excited modes with $\alpha = 1$, the numbers

$$k = n_0 + jm, \quad j = -5, -4, \dots, 5, 6, \quad m = 7, \quad (7)$$

and the signature $\{(-1)^j\}$. As shown in the inset, the transport corresponding to the initial state (7) goes from super-ballistic $D^2 \propto (\gamma t)^3$ to the ballistic regime. However, it should be noticed that eventually for large interacting times (for the case of the initial state (7) it is approximately for $\gamma t > 20$), the transport is diffusive.

VI. LOCALIZATION AND SCALING

Now let us demonstrate that the localization evidenced by the thin solid line in Fig. 1(b)) can also be scaled. I.e., by choosing the initial state one can extend the region of localization to an arbitrary degree. We illustrate this situation with the same initial state (5) as was used for Fig. 1(b)). I.e., we have four initially excited modes with numbers $k = n_0 - 2m, n_0, n_0 + 2m, n_0 + 4m$ and the signature $\{+, -, -, -\}$. Solid, dotted, dash-dotted and dashed lines correspond to $m = 1, 3, 4, 5$. One can see how the region of variance diminishing is extended toward the larger interaction times with extending the spatial localization of the initial state. One can see in Figs. (3)(b) that for the case of $m = 5$ the distribution of the probabilities $p_j(t)$ remains indeed well localized during all the interaction time. But eventually with increasing interaction time it comes to the usual diffusive regime, as it can be well seen for the solid and dotted lines.

VII. ANALYTIC MODEL

It is possible to derive a simple model giving an explanation of interference phenomena leading to the plethora of the observed regimes. To that end let us introduce the functions $\psi_{j,k} = (-1)^{j+k} g_{j,k}$ and consider the continuous approximation of an infinitely long chain getting from Eq.(2) 2D heat-transfer equation (Fick's second law of diffusion)²⁹:

$$\frac{1}{\gamma} \frac{\partial}{\partial t} \psi(x, y; t) = \frac{\partial^2}{\partial x^2} \psi(x, y; t) + \frac{\partial^2}{\partial y^2} \psi(x, y; t), \quad (8)$$

where x and y are normalized dimensionless spatial coordinates. We solve Eq.(8) with the following initial condition

$$\psi(x, y; 0) = \sum_{\forall jk} \phi_{jk} \delta(x - x_j) \delta(y - x_k),$$

where ϕ_{jk} describes initial excitation distribution of waveguides, and $\delta(x)$ is the Dirac delta-function. Thus, one can write down the standard solution for the continuous probability distribution²⁹:

$$p(x, t) = \sum_{\forall j, k} \frac{c_{jk}(t)}{\sqrt{2\pi\gamma t}} \exp \left\{ -\frac{(x - (x_j + x_k)/2)^2}{2\gamma t} \right\} \quad (9)$$

where $p(x, t) = \psi(x, x; t)$ and

$$c_{jk}(t) = \frac{\phi_{jk}}{\sqrt{8\pi\gamma t}} \exp \left\{ -\frac{(x_k - x_j)^2}{8\gamma t} \right\}. \quad (10)$$

Eqs.(9,10) lead to the following solution for the continuous version of the variance (4):

$$\bar{\Delta}^2(t) = \gamma t + D(t), \quad (11)$$

being the sum of the classical diffusive part and the interference part appearing due to coherence of the initial state

$$D(t) = \frac{1}{4\bar{p}_{tot}(t)} \sum_{\forall j, k} c_{jk}(t) (x_j + x_k)^2 - (\bar{x}(t))^2, \quad (12)$$

where the average displacement is

$$\bar{x}(t) = \frac{1}{2\bar{p}_{tot}(t)} \sum_{\forall j, k} c_{jk}(t) (x_j + x_k) \quad (13)$$

and the total probability

$$\bar{p}_{tot}(t) = \sum_{\forall j, k} c_{jk}(t). \quad (14)$$

VIII. DISCUSSION OF THE REGIMES

Eqs. (9-14) lead to simple explanation of the observed regimes discussed above. First of all, it is easy to see that deviations from the diffusive regime is indeed due to coherence of the initial state. In absence of the coherence, i.e., when $\phi_{jk} \propto \delta_{jj}$, the term $D(t)$ is constant and is zero for just one initially excited waveguide. This term is also constant asymptotically (for $\gamma t \rightarrow \infty$), if the sum of the initial state coherences is not zero $s_{coh} = \sum_{\forall j, k} \phi_{jk} \neq 0$.

It was already shown in Ref.³⁰, that having $s_{coh} = 0$ can lead to a number of quite nontrivial consequences. In particular, the choice of the initial state can lead to different kinds of the asymptotic polynomial decay of $p_{tot}(t)$.

Formally, it is quite easy to see from the long-time dynamics corresponding to $(x_k - x_j)^2/8\gamma t \rightarrow 0$, when the function $\sqrt{\gamma t} c_{jk}(t)$ can be approximated by the finite number of terms of the series

$$\sqrt{\gamma t} c_{jk}(t) \propto \sum_{n=0} \frac{\phi_{jk}}{n!} \left[-\frac{(x_k - x_j)^2}{8\gamma t} \right]^n \quad (15)$$

As it follows from Eqs. (9-15), for the initial state (5) having $s_{coh} = 0$ and $\sum_{\forall j, k} \phi_{jk} x_k x_j \neq 0$ leads to

$\sqrt{\gamma t} \bar{p}_{tot}(t \rightarrow \infty) \propto (\gamma t)^{-1}$ and $D(t \rightarrow \infty) = 2\gamma t$ giving rise to 3 times larger asymptotic diffusion rate observed in Figs. 1,2.

One can see also from Eqs. (9-15) that different polynomial decay laws of $p_{tot}(t)$ can be achieved by the choice of the initial state (5) zeroing first terms of the series (15) representing $p_{tot}(t)$. Such a choice of the initial state (5) will not change the asymptotically linear behaviour of $D(t \rightarrow \infty)$. However, it might affect the dynamics at initial times. Exactly this is shown in Figs. 2,3. Interference cancels lower-order terms making faster terms to appear and thus creating super-ballistic transport dynamics. In the localization case, interference can make $D(t)$ negative, as it is seen in Fig. 3.

Finally, Eqs. (9-15) clearly show time-scaling demonstrated in Figs. 2,3. Indeed, time-dependence of $D(t)$ is only through terms $(x_k - x_j)^2/\gamma t$. Having increased every distance $x_k - x_j$ m -times is equivalent to decreasing the dissipative coupling rate, γ , m^2 -times.

IX. REALISTIC SYSTEMS

The considered system of dissipatively coupled single-mode waveguides can be and is realized as an array of unitary coupled single-mode waveguides where every second waveguide is with an enhanced designed loss. Such system were realized by laser-writing waveguides in glass^{11,20,22,25}. They can be also realized, for example, on integrated photonic platforms, such as InP platform^{27,37}. The latter realization is depicted in Fig. 4(a), where the coupling between waveguides is with the coupling constant v , and every second waveguide is subject to the designed loss with the rate Γ . This scheme can be described by the following master equation for the total density matrix of the system

$$\begin{aligned} \frac{d}{dt} \rho_{tot} = & -\frac{i}{\hbar} [H, \rho_{tot}] + \\ & \Gamma \sum_{\forall j} \left(2b_j \rho_{tot} b_j^\dagger - \rho_{tot} b_j^\dagger b_j - b_j^\dagger b_j \rho_{tot} \right), \end{aligned} \quad (16)$$

where the modal interaction Hamiltonian is

$$H = \sum_{\forall j} \hbar v \left(b_j^\dagger (a_j + a_{j+1}) + (a_j^\dagger + a_{j+1}^\dagger) b_j \right), \quad (17)$$

with b_j , b_j^\dagger denoting the annihilation and creation operators for the lossy waveguides. In the limit of large loss

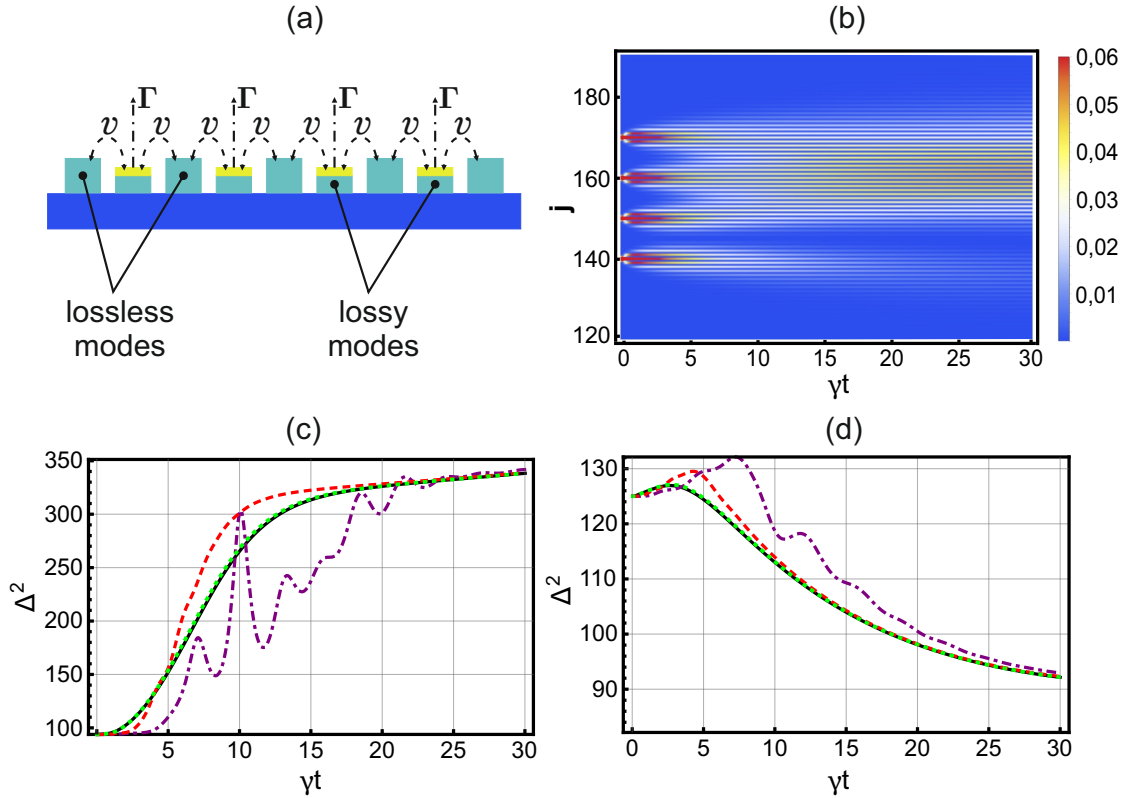


FIG. 4. (a) The scheme of tight-binding periodic system of coupled single-mode waveguides with each second waveguide being lossy described by the master equation (17,17). (b) Distribution of the population p_j for all the waveguides including lossy ones and for the initial state corresponding to the dashed line in Fig. 3(a). (c,d) Variance for the states given by the solution of Eqs.(17,17) for the initial state of the a_j modes the same as for the dash-dotted line in Fig. 2(a,c) and dashed line in Fig. 3(a,d). The initial states of the modes b_j are the vacuum. Dash-dotted, dashed and dotted lines correspond to $v/\Gamma = 0.43, 0.25, 0.083$. Solid line replicate dash-dotted line in Fig. 2(a) (c) and dashed line in Fig. 3(a) (d).

$v/\Gamma \rightarrow 0$, the lossy modes b_j can be adiabatically eliminated giving rise to the master equation (1) with the dissipative coupling rate $\gamma = 4v^2/\Gamma$ only for the modes a_j (for the detailed derivation see, for example, Ref.³⁸).

Notice that such a system discussed in Ref.²⁰ for a single initially excited waveguide demonstrated appearance of the diffusive regime typical for the dissipatively coupled bosonic chains discussed here with the transition time of about $\gamma t \sim 1$. However, the waveguide system of Ref.²⁰ was actually far from the regime of purely dissipative coupling realized in the limit $v/\Gamma \rightarrow 0$. Figs. 4(c,d) shows how for the realistic structure of Fig. 4(a) the dissipative coupling limit is approached for the super-ballistic regime (Fig. 4(c)) and localization (Fig. 4(d)) regime with diminishing the ratio v/Γ while keeping γ constant. Dashed, dotted and dash-dotted lines in Figs. 4(c) were obtained for the initial state (5) with excitation as was for the dash-dotted line in Fig. 2(a). Dashed, dotted and dash-dotted lines in Figs. 4(d) were obtained for the initial state (5) with excitation as was for the dashed line in Fig. 3(a). For both the panels 4(c,d) dash-dotted, dashed

and dotted lines correspond to $v/\Gamma = 0.43, 0.25, 0.083$. All the b_j modes were supposed initially in the vacuum states. Solid lines in Figs. 4(c,d) show corresponding solutions of Eq.(1).

It can be seen in Figs. 4(c,d) that the limit of large loss is actually quite easily reached in practice. Already for $v \approx 0.25\Gamma$ one has a good approximation of the dissipative coupling regime, and $v \approx 0.08\Gamma$ gives practically coinciding results with ones obtained from Eq.(1). The panel Fig. 4(b) shows the normalized population distribution, p_j , in all the waveguides including lossy ones for the localization regime corresponding to the dotted line in Fig. 4(d). As it should be expected in the regime of the dissipative coupling, population in the lossy waveguides drops very quickly (on the scale of $\Gamma t \sim 1$) reproducing the picture seen in Fig. 3 (c).

X. CONCLUSIONS

Here we have demonstrated that perfectly periodic networks of dissipatively coupled bosonic modes can exhibit a variety of transport regimes in dependence on the initial excitation of the modes. We have shown that coherent interference effects can lead to super-ballistic transport regime or to localization in any predefined interaction time interval. This interval can be extended by changing the initial state. We have described the way of doing that and derived a simple analytic model to explain such scaling behaviour. This model also explains appearance both localization and super-ballistic regimes, and demonstrates the nature of different possible rates of the asymptotic transport regime. It is always diffusive. However, for certain initial states the rate of diffusion can be three times more than for others.

Notice that here we have pursued only the task of demonstrating possibilities offered by interference occurring in the coherent diffusive quantum walk of ampli-

tudes. We have discussed transport regimes for a different but classical states factorized states of the bosonic modes. We have not exploited correlated states and propagation of correlation and nonclassicality through our network. To provide a hint toward possible non-trivial effects connected with quantum correlation transport, one can notice that the finite system described by Eq.(1) has entangled stationary states^{25,30}. Also, dynamics of n -th order correlation function describes coherent diffusion in n -dimensions.

The discussed regimes can be observed in tight-bonding 1D systems of coupled single-mode waveguides feasible in different photonic platforms. Such systems were already realized by laser-writing in bulk glass, and can be also realized with integrated photonic platforms.

The authors (D.M and I.P) gratefully acknowledge support from the BRFFI projects F21KOP-002 and F22B-008. G.S. acknowledges supports from the Horizon 2020 project TERASSE 823878. and from the NATO project NATO SPS - G5860.

¹ Y. Aharonov, L. Davidovich, and N. Zagury. Quantum random walks. *Phys. Rev. A*, 48:1687–1690, Aug 1993.

² J Kempe. Quantum random walks: An introductory overview. *Contemporary Physics*, 44(4):307–327, 2003.

³ VIV Kendon. Decoherence in quantum walks – a review. *Mathematical Structures in Computer Science*, 17 (6):1169–1220, 2007.

⁴ Salvador Venegas-Andraca. Quantum walks: A comprehensive review. *Quantum Information Processing*, 11, 01 2012.

⁵ Edward Farhi and Sam Gutmann. Quantum computation and decision trees. *Phys. Rev. A*, 58:915–928, Aug 1998.

⁶ Oliver Mülken and Alexander Blumen. Continuous-time quantum walks: Models for coherent transport on complex networks. *Physics Reports*, 502(2):37–87, 2011. ISSN 0370-1573.

⁷ Hagai B. Perets, Yoav Lahini, Francesca Pozzi, Marc Sorel, Roberto Morandotti, and Yaron Silberberg. Realization of quantum walks with negligible decoherence in waveguide lattices. *Phys. Rev. Lett.*, 100:170506, May 2008.

⁸ Oliver Mülken, Alexander Blumen, Thomas Amthor, Christian Giese, Markus Reetz-Lamour, and Matthias Weidmüller. Survival probabilities in coherent exciton transfer with trapping. *Phys. Rev. Lett.*, 99:090601, Aug 2007.

⁹ Patrick Rebentrost, Masoud Mohseni, and Alán Aspuru-Guzik. Role of quantum coherence and environmental fluctuations in chromophoric energy transport. *The Journal of Physical Chemistry B*, 113(29):9942–9947, 2009.

¹⁰ A. Chia, K. C. Tan, Ł. Pawela, P. Kurzyński, T. Paterek, and D. Kaszlikowski. Coherent chemical kinetics as quantum walks. i. reaction operators for radical pairs. *Phys. Rev. E*, 93:032407, Mar 2016.

¹¹ Markus Gräfe, René Heilmann, Maxime Lebugle, Diego Guzman-Silva, Armando Perez-Leija, and Alexander Szameit. Integrated photonic quantum walks. *Journal of Optics*, 18(10):103002, sep 2016.

¹² Liad Levi, Mikael Rechtsman, Barak Freedman, Tal Schwartz, Ofer Manela, and Mordechai Segev. Disorder-enhanced transport in photonic quasicrystals. *Science*, 332 (6037):1541–1544, 2011.

¹³ Liad Levi, Yevgeny Krivolapov, Shmuel Fishman, and Mordechai Segev. Hyper-transport of light and stochastic acceleration by evolving disorder. *Nature Physics*, 8 (12):912–917, December 2012.

¹⁴ Zhenjun Zhang, Peiqing Tong, Jiangbin Gong, and Baowen Li. Quantum hyperdiffusion in one-dimensional tight-binding lattices. *Phys. Rev. Lett.*, 108:070603, Feb 2012.

¹⁵ A. S. Pikovsky and D. L. Shepelyansky. Destruction of anderson localization by a weak nonlinearity. *Phys. Rev. Lett.*, 100:094101, Mar 2008.

¹⁶ Philip Held, Melanie Engelkemeier, Syamsundar De, Sonja Barkhofen, Jan Sperling, and Christine Silberhorn. Driven gaussian quantum walks. *Phys. Rev. A*, 105:042210, Apr 2022.

¹⁷ A. Schreiber, K. N. Cassemiro, V. Potoček, A. Gábris, I. Jex, and Ch. Silberhorn. Decoherence and disorder in quantum walks: From ballistic spread to localization. *Phys. Rev. Lett.*, 106:180403, May 2011.

¹⁸ Gunter M. Schütz and Steffen Trimper. Elephants can always remember: Exact long-range memory effects in a non-markovian random walk. *Phys. Rev. E*, 70:045101, Oct 2004.

¹⁹ A. Romanelli, R. Siri, G. Abal, A. Auyuanet, and R. Donangelo. Decoherence in the quantum walk on the line. *Physica A: Statistical Mechanics and its Applications*, 347: 137–152, 2005. ISSN 0378-4371.

²⁰ T Eichelkraut, R Heilmann, Steffen Weimann, Simon Stützer, F Dresow, D Christodoulides, Stefan Nolte, and Alexander Szameit. Mobility transition from ballistic to diffusive transport in non-hermitian lattices. *Nature communications*, 4:2533, 09 2013.

²¹ M. Golshani, S. Weimann, Kh. Jafari, M. Khazaei Nezhad, A. Langari, A. R. Bahrampour, T. Eichelkraut, S. M. Mah-

davi, and A. Szameit. Impact of loss on the wave dynamics in photonic waveguide lattices. *Phys. Rev. Lett.*, 113:123903, Sep 2014.

²² M. Golshani, S. Weimann, Kh. Jafari, M. Khazaei Nezhad, A. Langari, A. R. Bahrampour, T. Eichelkraut, S. M. Makhadavi, and A. Szameit. Impact of loss on the wave dynamics in photonic waveguide lattices. *Phys. Rev. Lett.*, 113:123903, Sep 2014.

²³ A. R. R. Carvalho, P. Milman, R. L. de Matos Filho, and L. Davidovich. Decoherence, pointer engineering, and quantum state protection. *Phys. Rev. Lett.*, 86:4988–4991, May 2001.

²⁴ A. Metelmann and A. A. Clerk. Nonreciprocal photon transmission and amplification via reservoir engineering. *Phys. Rev. X*, 5:021025, Jun 2015.

²⁵ S. Mukherjee, D. Mogilevtsev, G. Slepyan, Thomas H. Doherty, R. Thomson, and N. Korolkova. Dissipatively coupled waveguide networks for coherent diffusive photonics. *Nature Communications*, 8:1909, 2017.

²⁶ M. Thornton, A. Sakovich, A. Mikhalychev, J. D. Ferrer, P. de la Hoz, N. Korolkova, and D. Mogilevtsev. Coherent diffusive photon gun for generating nonclassical states. *Phys. Rev. Applied*, 12:064051, Dec 2019.

²⁷ I. Peshko, D. Pustakhod, and D. Mogilevtsev. Breaking reciprocity by designed loss. *J. Opt. Soc. Am. B*, 39(7):1926–1935, Jul 2022.

²⁸ C. Arenz and A. Metelmann. Emerging unitary evolutions in dissipatively coupled systems. *Phys. Rev. A*, 101:022101, Feb 2020.

²⁹ Gregory F. Lawler. *Random walk and the heat equation* / Gregory F. Lawler. Student mathematical library ; v. 55. American Mathematical Society, Providence, 2010. ISBN 9780821848296.

³⁰ D. Mogilevtsev, G. Ya. Slepyan, E. Garusov, S. Ya. Kilin, and N. Korolkova. Quantum tight-binding chains with dissipative coupling. *New Journal of Physics*, 17(4):043065, apr 2015.

³¹ Ronen Chriki, Slava Smartsev, David Eger, Ofer Firstenberg, and Nir Davidson. Coherent diffusion of partial spatial coherence. *Optica*, 6(11):1406–1411, Nov 2019.

³² Slava Smartsev, Ronen Chriki, David Eger, Ofer Firstenberg, and Nir Davidson. Structured beams invariant to coherent diffusion. *Opt. Express*, 28(22):33708–33717, Oct 2020.

³³ Yanhong Xiao, Mason Klein, Michael Hohensee, Liang Jiang, David F. Phillips, Mikhail D. Lukin, and Ronald L. Walsworth. Slow light beam splitter. *Phys. Rev. Lett.*, 101:043601, Jul 2008.

³⁴ O. Firstenberg, P. London, D. Yankelev, R. Pugatch, M. Shuker, and N. Davidson. Self-similar modes of coherent diffusion. *Phys. Rev. Lett.*, 105:183602, Oct 2010.

³⁵ Denis S. Grebenkov. Nmr survey of reflected brownian motion. *Rev. Mod. Phys.*, 79:1077–1137, Aug 2007.

³⁶ J. M. Kikkawa and D. D. Awschalom. Lateral drag of spin coherence in gallium arsenide. *Nature*, 397(6715):139–141, January 1999.

³⁷ L. M. Augustin, R. Santos, E. den Haan, S. Kleijn, P. J. A. Thijs, S. Latkowski, D. Zhao, W. Yao, J. Bolk, H. Ambrosius, S. Mingaleev, A. Richter, A. Bakker, and T. Korthorst. InP-Based Generic Foundry Platform for Photonic Integrated Circuits. *IEEE J. Sel. Topics in Quantum Electron.*, 24(1):1–10, Jan 2018. ISSN 1077-260X.

³⁸ D. Mogilevtsev and V. S. Shchesnovich. Single-photon generation by correlated loss in a three-core optical fiber. *Opt. Lett.*, 35(20):3375–3377, Oct 2010.